Typhoon Kai-Tak: An Ocean's Perfect Storm

TZU-LING CHIANG AND CHAU-RON WU

Department of Earth Sciences, National Taiwan Normal University, Taipei, Taiwan

LIE-YAUW OEY

Program in Atmospheric and Oceanic Sciences, Princeton University, Princeton, New Jersey

(Manuscript received 15 June 2010, in final form 25 August 2010)

ABSTRACT

An unusually intense sea surface temperature drop (ΔSST) of about 10.8°C induced by the Typhoon Kai-Tak is observed in the northern South China Sea (SCS) in July 2000. Observational and high-resolution SCS model analyses were carried out to study the favorable conditions and relevant physical processes that cause the intense surface cooling by Kai-Tak. Upwelling and entrainment induced by Kai-Tak account for 62% and 31% of the ΔSST, respectively, so that upwelling dominates vertical entrainment in producing the surface cooling for a subcritical storm such as Kai-Tak. However, wind intensity and propagation speed alone cannot account for the large ΔSST. Prior to Kai-Tak, the sea surface was anomalously warm and the main thermocline was anomalously shallow. The cause was a delayed transition of winter to summer monsoon in the northern SCS in May 2000. This produced an anomalously strong wind stress curl and a cold eddy capped by a thin layer of very warm surface water west of Luzon. Kai-Tak was the ocean's perfect storm in passing over the eddy at the ''right time,'' producing the record SST drop and high chlorophyll-a concentration.

1. Introduction

Cold sea surface temperatures (SST) in the wake of tropical cyclones (TC) are well known. The combined action of upwelling and entrainment (vertical mixing) induced by TC brings deep cold waters to the sea surface, producing cold patches with SSTs several degrees cooler than the ambient waters. The maximum SST drop (ΔSST) caused by TCs could be as much as 5°–6°C but rarely exceeds 6°C (Wentz et al. 2000). In July 2000, however, an unusually intense surface cooling of about 10.8°C was observed in the northern South China Sea (SCS). The extreme cooling was induced by a relatively weak typhoon, Kai-Tak (3–11 July 2000), a category-1 typhoon on the Saffir–Simpson hurricane scale with a maximum wind speed of 38.6 m s^{-1} and a minimum central pressure of 965 hPa. Lin et al. (2003) reported that Kai-Tak triggered a 30-fold increase in surface chlorophyll-a concentration and that this single event alone could account for 2%–4% of the annual new production in the SCS. We will show that the extreme ocean cooling and high chlorophyll-a concentration by Kai-Tak were due to a unique combination of its slow propagation speed and favorable climatic and oceanic conditions prior to the storm's arrival. For this reason, we call Kai-Tak the ocean's perfect storm.

Excluding Kai-Tak, between 1958 and 2008, the maximum SST cooling caused by 31 other typhoons ranges from 1° to 8°C (Fig. 1). The average of maximum cooling is about 4.31° ± 2.03°C. The cooling induced by Kai-Tak is nearly three standard deviations from the mean. Figure 1 suggests that the maximum cooling is inversely related to the storm's propagation speed U, but that is not the only factor. Our goal is to explain why Kai-Tak can induce such a large SST drop.

Kai-Tak formed off the northwestern Luzon Island at ~15.7°N, 118.1°E on 3 July 2000. It moved northeastward and turned northwestward near 18.8°N, 120.9°E on 5 July (Fig. 2c). During 6–7 July, the track of Typhoon Kai-Tak may have been affected by Typhoon Kirogi (2–9 July 2000), a fast, northward-moving category-4 typhoon that formed approximately 1000 km east of Philippines (outside the domain shown in Fig. 2). However, during that time, Typhoon Kirogi had weakened to category 1; on 8–9 July, when Typhoon Kai-Tak produced the largest

Corresponding author address: Chau-Ron Wu, Department of Earth Sciences, National Taiwan Normal University, 88, Section 4 Ting-Chou Road, Taipei 11677, Taiwan.
E-mail: cwu@ntnu.edu.tw

DOI: 10.1175/2010JPO4518.1

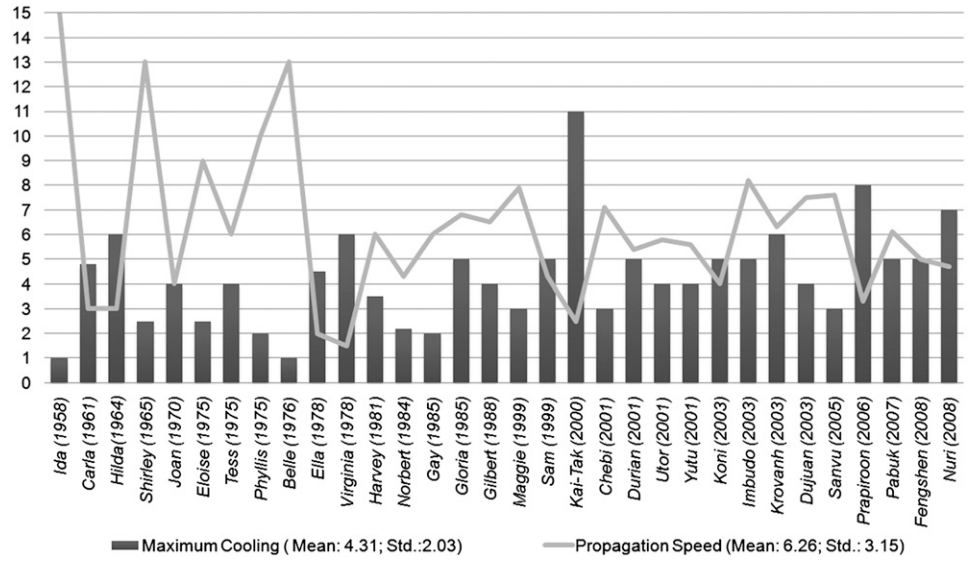

FIG. 1. Maximum cooling (°C) and propagation speed (m s^{-1}) of typhoons. The 1958–88 period in various regions is from Bender et al. (1993). The 1998–2008 period is for the northern SCS: maximum cooling from TMI images and propagation speed from JTWC best-track data.

drop in SST in the SCS, Typhoon Kirogi was some 3000–4000 km away off the northeastern coast of Honshu and Hokkaido, Japan, and was further downgraded to the tropical storm status. The impact of Typhoon Kirogi on the ΔSST by Kai-Tak is therefore expected to be very small. From 6 to 8 July, Kai-Tak lingered and traced an anticlockwise loop around 20°N, 119°E. Kai-Tak began to move rapidly northward after 8 July and finally made landfall at the eastern coast of Taiwan on 9 July. Figures 2a,b are pre-Kai-Tak (2 July 2000) and post-Kai-Tak (9 July 2000) daily SST images (ascending) from the Tropical Rainfall Measuring Mission Microwave Imager (TMI). The minimum SST after the typhoon was 20.3°C at 20.1°N, 119.1°E, whereas the SST at the same location before the typhoon was 31.1°C, leading to a maximum SST drop of ~10.8°C (Fig. 2c). The area of intense surface cooling (SST drop > 9°C) is about 1° × 1° (19.5°–20.5°N, 118.8°–119.8°E). The cooling is caused by upwelling and mixing, which also bring nutrient-rich subsurface waters up to the mixed layer and increase the surface chlorophyll-a concentration (Lin et al. 2003; Wu et al. 2008).

Price (1981) suggested that entrainment is the primary mechanism that decreases the SST. In addition, for a slow-moving typhoon, strong upwelling may also reduce the SST. In the case of Kai-Tak, the maximum Ekman pumping estimated from the QuikSCAT–NCEP blended wind on 7 July is large, about 10^{-3} m s^{-1}. However, wind intensity and propagation speed alone cannot account for the drastic SST drop induced by Kai-Tak. Bender et al. (1993) categorized three groups of SST cooling based on 16 tropical cyclones in various regions according to their propagation speeds: slow (<4 m s^{-1}), medium (4–8 m s^{-1}), and fast (>8 m s^{-1}). The corresponding averaged maximum ΔSSTs are 5.3°, 3.5°, and 1.8°C, respectively. The maximum ΔSSTs due to various typhoons in the northern SCS (Fig. 1) fall roughly into Bender et al.'s categories and criteria. Typhoon Kai-Tak with ΔSST = 10.8°C was one of only four storms [the others were Hilda (1964; ~6°C), Virginia (1978; ~6°C), and Prapiroon (2006; ~8°C)] in the slow-storm category that has maximum SST drops exceeding Bender et al.'s criteria of ΔSST = 5.3°C.

There are several model studies that investigate the oceanic responses due to typhoons in the SCS. Chu et al. (2000) used the Princeton Ocean Model (POM) together with the Tropical Cyclone Wind Profile Model (TCWPM) to study the response to Typhoon Ernie (1996). They found strong similarities between open-ocean and coastal responses, including significant SST cooling, subsurface intense upwelling, and cooling at the base of the mixed layer. Jiang et al. (2009) developed a three-dimensional, coupled air–sea model [the fifth-generation Pennsylvania State University–NCAR Mesoscale Model (MM5) and POM] to study the upper-ocean response to Typhoon Krovanh (2003). They found that the SST cooling is mainly caused by entrainment. These numerical studies have provided good insights, and they emphasize more on model development and accuracy of the simulation when compared against observations.

In this work, a fine-resolution SCS model driven by satellite wind product is used to understand the various mechanisms that could cause the intense SST cooling by

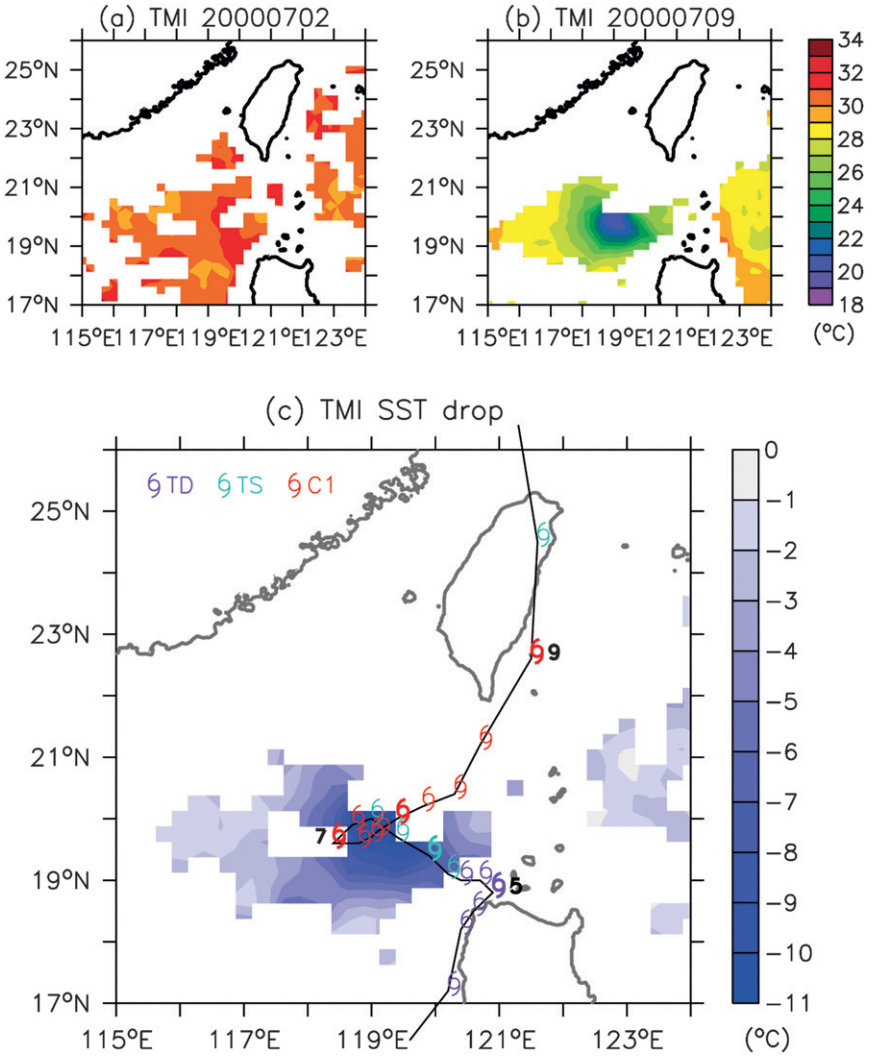

FIG. 2. The TMI daily SST images (ascending) from TMI on (a) 2 and (b) 9 Jul. (c) SST drop between 2 and 9 Jul with Kai-Tak track with selected dates indicated and intensity marked 6-hourly from the JTWC best-track data.

Kai-Tak. The outline of the paper is as follows: Section 2 describes the observations and numerical model used in this study. The results, including analyses of the relative importance of upwelling and entrainment, and the effects of background thermal structure and propagation speed are given in section 3. In section 4, we discuss the climatic and oceanic conditions that led to the strong SST drop. Section 5 concludes the paper.

2. Observations and model description

The SST data from the ¼° × ¼° TMI (available online at http://www.remss.com) are used to verify the decrease in SST due to Typhoon Kai-Tak. The intensity and track of Kai-Tak are obtained from the best-track data of the Joint Typhoon Warning Center (JTWC; available online at http://www.usno.navy.mil/JTWC). The wind data are from the high temporal and spatial resolution (6-hourly and 0.5° × 0.5°) datasets from the QuikSCAT–NCEP blended wind product [National Center for Atmospheric Research (NCAR) Data Support Section (DSS); available online at http://dss.ucar.edu; Milliff et al. 1999]. The gridded geostrophic velocity (GSV) is from the Archiving, Validation and Interpretation of Satellite Oceanographic data (AVISO; available online at http://www.aviso.oceanobs.com). They are merged from five altimeter missions—*Envisat*, *European Remote Sensing Satellite-1* (*ERS-1*) and *ERS-2*, *Geosat Follow-On* (*GFO*), *Jason-1*, and Ocean Topography Experiment (TOPEX)/Poseidon—and have resolutions of 0.25° in space and 7 days in time.

The SCS model used in this study is based on the sigma-coordinate POM (Mellor 2004). The three-dimensional,

TABLE 1. List of experiments.

Case	Wind forcing	Thermal structure	Note	SST drop (°C)
CTL	2000 (Kai-Tak)	2000: July	Control run	10.3
EX1	2000 (Kai-Tak)	2000: July	$K_M = 0.003$ and $K_H = 0.0037$ m^2 s^{-1}	6.4
EX2	2000 (Kai-Tak)	2000: July	1D	3.2
EX3	2000 (Kai-Tak)	2001: July	—	5.9
EX4	2000 (Kai-Tak)	*WOA01*: June	—	7.2
EX5	2001 (Utor)	2000: July	—	6.7
EX6	2001 (Utor)	2000: July	1-day stop on 5 Jul	9.5

free surface model solves the primitive equations for momentum, salt, and heat. The model domain extends from 99° to 124°E in longitude and from 2° to 27°N in latitude. The horizontal grid size is $^1/_{16}$° and there are 26 sigma levels in the vertical. A larger-scale East Asian Marginal Seas model (Hsin et al. 2008) is used to specify the open boundary condition of the SCS model at a daily time interval. The SCS model is driven by the 6-hourly 0.5° × 0.5° QuikSCAT–NCEP blended wind product (Milliff et al. 1999) and is nudged at the sigma grid nearest to the sea surface by the weekly 1° Advanced Very High Resolution Radiometer (AVHRR) SST data (NCAR DSS). The SCS model has been validated by the observed temperature from a long-term mooring in the northern SCS as well as current velocity data from several mooring stations in the SCS. These validations and more detailed descriptions of the SCS model are given in Wu and Chiang (2007) and Chiang et al. (2008). For the present study, we use the results from 1 July 2000 and 1 July 2001 as initial conditions in the later experiments. All experiments are carried out using the same SCS model but with a different model setup (see Table 1). More details of these experiments will be separately described below.

At high wind speeds, the commonly used wind drag formula (e.g., Large and Pond 1981; Trenberth 1989) that increases linearly with wind speed is not valid. If it is used, the SST drop by typhoon is usually overestimated in the simulations. Thus, we adopt the drag formula that fits Large and Pond's formula at low wind speed and Powell et al. (2003) at high wind speeds (see Oey et al. 2006):

$$
\begin{aligned}
C_d \times 10^{-3} &= 1.2, && W \le 11\ (\mathrm{m\,s^{-1}});\\
&= 0.49 + 0.065W, && 11 < W \le 19\ (\mathrm{m\,s^{-1}});\\
&= 1.364 + 0.0234W - 0.00023158W^2, && 19 < W \le 100\ (\mathrm{m\,s^{-1}}),
\end{aligned} \tag{1}
$$

where W is the wind speed.

The present study uses only one single model (the SCS model, which is based on POM). To simulate the ocean response due to Typhoon Kai-Tak, we first derive a near-realistic initial state by nudging satellite SST data during the spinup stage, as described above. We then use this same initial state to continue for one month without any SST nudging all typhoon-induced ocean response experiments. Because the satellite SST is not used in these experiments, the temperature drop is produced only by the internal dynamics of the numerical ocean model.

3. Results

a. Kai-Tak simulation

Figure 3 shows daily averaged SST and surface velocity from the control run (CTL). Before the tropical depression (2 July; Fig. 3a), SST contours are approximately oriented from northeast to southwest with lower temperatures near the Chinese coast. The tropical depression formed on 5 July (Fig. 3b) and turned northwestward near 18.8°N, 120.9°E. The SST decreases near the northwestern Luzon Island coast. Kai-Tak intensified and became a category-1 typhoon on 7 July, when it lingered near 19.6°N, 118.4°E (Fig. 3c). The SST on 9 July (Fig. 3d) displays the largest temperature drop over the Kai-Tak's duration. A comparison of the modeled SST and ΔSST (9 July minus 2 July) in Fig. 3 with the corresponding TMI images in Fig. 2 shows good agreement. The maximum SST cooling of ~10.3°C (Fig. 3e) is near 19.9°N, 119.4°E.

b. Relative importance of upwelling and entrainment

As Price (1981) suggested, for a slow-moving cyclone, strong upwelling together with entrainment mixing may significantly decrease the SST. The relative importance of upwelling and entrainment in realistic simulations of

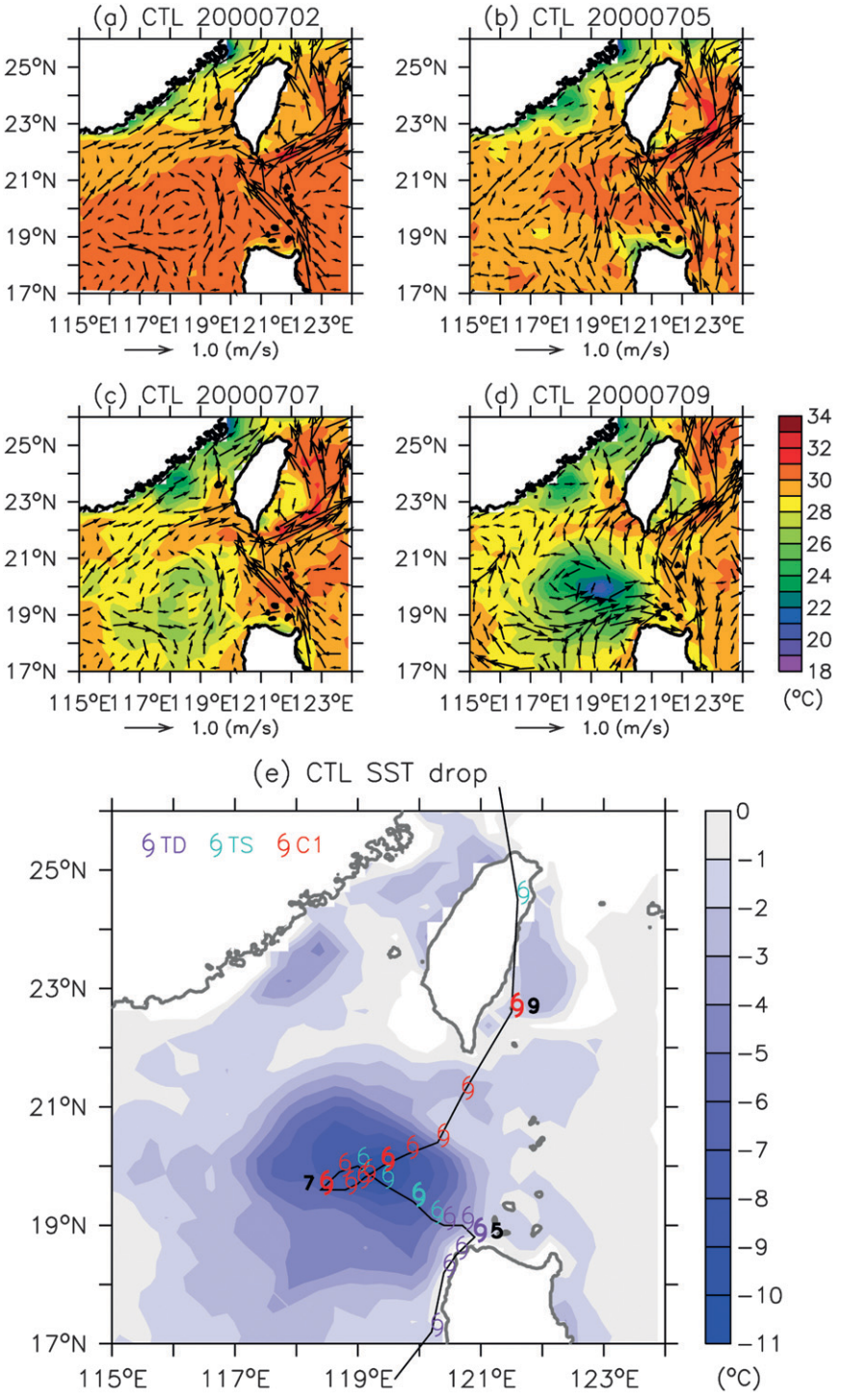

FIG. 3. Daily averaged SST and surface velocity (0–50 m) from CTL on (a) 2, (b) 5, (c) 7, and (d) 9 Jul. (e) CTL SST drop between 2 and 9 Jul with Kai-Tak track with selected dates indicated and intensity from the JTWC best-track data.

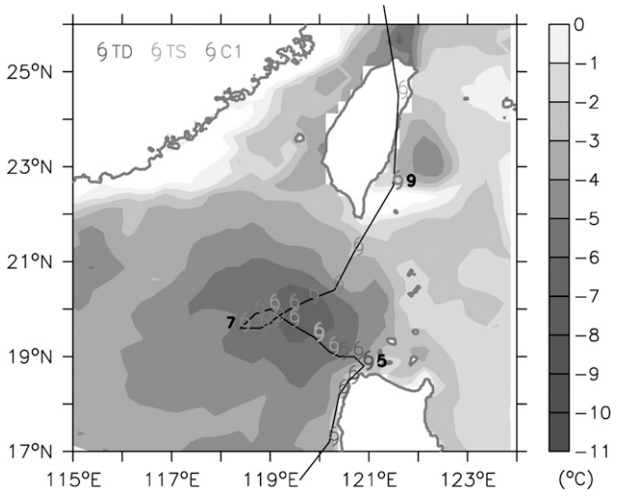

FIG. 4. The SST drop for EX1 between 2 and 9 Jul with Kai-Tak track with selected dates indicated and intensity from the JTWC best-track data.

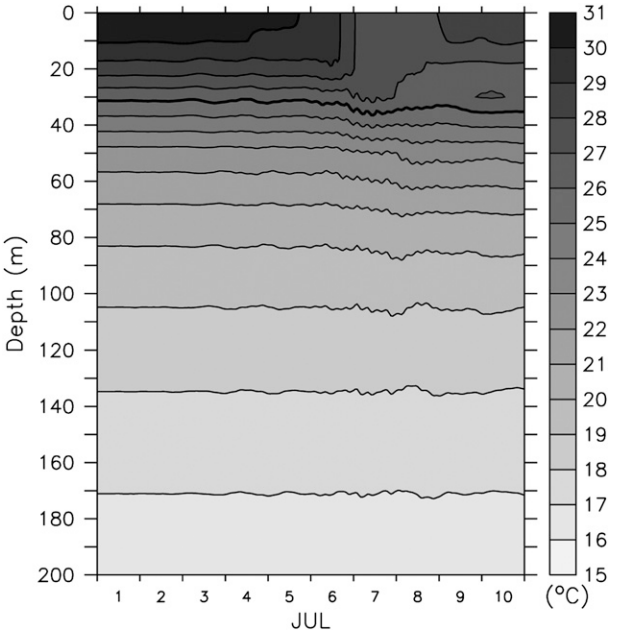

FIG. 5. The time–depth contours of temperature for EX2 (D26 showed by thick line).

ocean response to tropical cyclones is rarely estimated because of the inherent difficulty in separating the two processes. Here, two experiments are conducted to evaluate the relative importance of these two processes. Experiment 1 (EX1; see Table 1) is an upwelling experiment. We set the values of vertical kinematic viscosity K_M and vertical diffusivity coefficient K_H to be constants = 0.003 and 0.0037 $m^2\ s^{-1}$, respectively. These are the smallest values chosen to keep the model numerically stable under the strong winds. The chosen K_H value is about two orders of magnitude smaller than typical values found in CTL during Kai-Tak and ensures that entrainment is small in this experiment. The other model parameters and forcing remain unchanged. Because Ekman pumping is independent of K_M, this experiment therefore simulates the upwelling component of the cooling process. Other temperature fluctuations caused by horizontal variations (e.g., mesoscale eddies, near-inertial internal waves, etc.) are also included (Oey et al. 2008). However, eddies generally evolve at longer time scales than typhoon-induced ocean response, and inertial waves are reduced by the daily averaging that we apply to the model results. Figure 4 shows that the ΔSST pattern in EX1 is similar to that in CTL, but with a weaker magnitude. The maximum ΔSST in EX1 is at the same location as in CTL ~(19.9°N, 119.4°E) and is about 6.4°C. We have repeated this experiment (EX1) by doubling the values of K_M and/or K_H, and the results are virtually identical to Fig. 4, suggesting that the chosen K_H is sufficiently small and that the upwelling is largely independent of K_M.

Experiment 2 (EX2; see Table 1) is designed to simulate entrainment only. To eliminate upwelling caused by Ekman pumping, a one-dimensional (1D) numerical model is used. The 1D model is identical to the three-dimensional (3D) SCS model, except that only the vertical structure is solved. Thus, the Mellor–Yamada turbulence closure submodel and the treatment of vertical advection and diffusion are identical with the 3D SCS model. The initial temperature and salinity on 1 July 2000 are taken from the corresponding CTL profiles at 20°N, 119°E, near where the maximum ΔSST was observed. The 1D model has the advantage of not only eliminating effects of upwelling by Ekman pumping, but it also eliminates other temperature fluctuations related to horizontal variations, (e.g., eddies, near-inertial internal waves, etc.). In other words, EX2 simulates purely the vertical entrainment and mixing processes. Figure 5 shows the time–depth contours of temperature for EX2. The ΔSST in EX2 is about 3.2°C, compared to ΔSST = 10.3°C for CTL. This smaller SST drop indicates that 1D model is not sufficient for investigating the SST cooling induced by a slow-moving tropical cyclone. The result shown in this realistic simulation is consistent with that in Yablonsky and Ginis (2009), who conducted several idealized experiments using both 1D and 3D models to investigate SST cooling due to hurricane forcing.

Therefore, 62% (6.4°C) and 31% (3.2°C) of the SST drop by Kai-Tak are caused by upwelling and entrainment, respectively. In the case of Typhoon Kai-Tak, upwelling dominates vertical entrainment in producing the simulated intense surface cooling. The upwelling

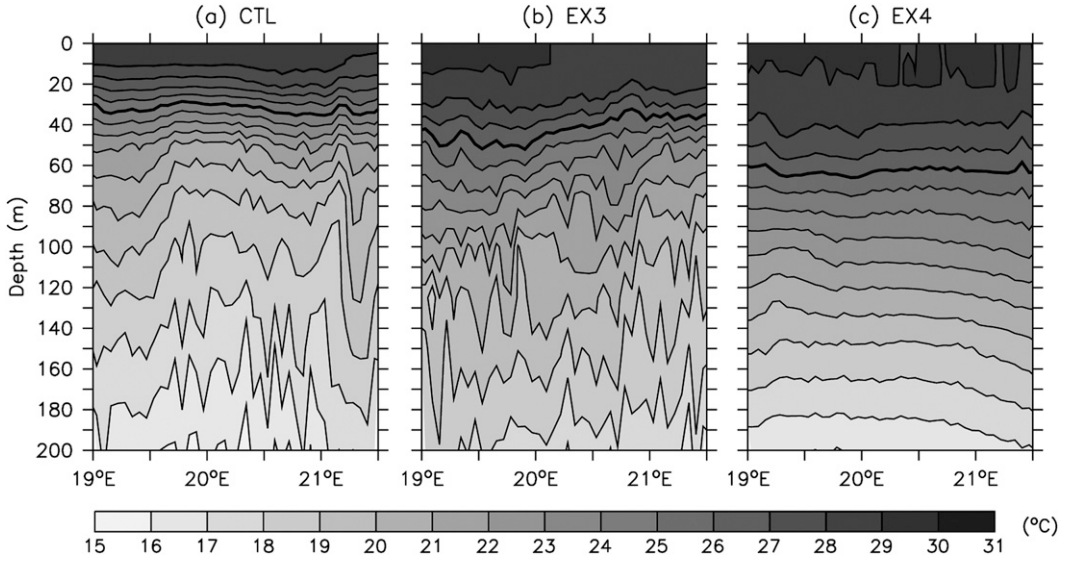

FIG. 6. Initial temperature structures in the upper 200 m at 119°E for (a) CTL, (b) EX3, and (c) EX4 (D26 showed by thick line).

experiment (EX1) and entrainment experiment (EX2) together account for 93% of the total ΔSST. As mentioned above, the two processes interact and there also exist other processes. Nonetheless, the close agreement of the summed (i.e., upwelling + entrainment) contribution to ΔSST to the control experiment's ΔSST indicate (i) that the two contributions are dominant and (ii) that our designs of EX1 and EX2 to separate them are appropriate.

When Kai-Tak was at 20°N, 119°E from 1800 UTC 6 July to 0000 UTC 8 July, its propagation speed was 0.65–1.96 m s^{-1}. The first-mode baroclinic phase speed computed using the July temperature and salinity profiles from the *World Ocean Atlas 2001* (*WOA01*) is ~2 m s^{-1}, so Kai-Tak's propagation was subcritical during this period. Localized upwelling is prevalent under a subcritical storm, whereas lee waves with alternating upwelling and downwelling cells are left behind a supercritical storm (Geisler 1970). Strong upwelling is often observed under slowly moving (subcritical) storms (e.g., Price 1981; Oey et al. 2006, Oey et al. 2007). However, a ΔSST of more than 10°C, such as that occurred after Kai-Tak, is uncommon. There may therefore be other factor(s) involved in the excessive cooling.

The excessive cooling is most likely due to the unusual upper-ocean state of summer 2000. The reason for this will be explained in section 4. Here we compare in Fig. 6 the temperature structures at 119°E on 1 July 2000 (for the CTL experiment; Fig. 6a), 1 July 2001 (i.e., a different year; Fig. 6b), and (c) June climatological temperature (and salinity) from *WOA01* (Conkright et al. 2002). In 2000 (Fig. 6a), the near-surface temperature is 1°–2°C warmer than in 2001 (Fig. 6b) and than in climatology (Fig. 6c). The thermocline in 2000 is 20–80 m shallower, so that the corresponding depth of the 26°C isotherm (D26) is the thinnest among the three temperatures. Near 20°N, 119°E (location of maximum SST drop due to Kai-Tak), for example, the 19°–20°C isotherms are at $z \approx 85$ m in CTL but are depressed to depths of $z \approx 155$ and 140 m in Figs. 6b,c, respectively.

c. *Effects of background thermal structure and propagation speed*

It is well known that a tropical cyclone over a shallow thermocline tends to produce larger cooling (e.g., Price 1981). Appendix A confirms this with two experiments, EX3 and EX4, initialized with the SCS model's 1 July 2001 field (Fig. 6b) and *WOA01* June climatology (Fig. 6c), respectively. The maximum ΔSSTs are 5.9° and 7.2°C, respectively, both weaker than the CTL ΔSST of 10.3°C.

Appendix A also describes two other experiments (EX5 and EX6; Table 1) that test the sensitivity of ΔSST on the typhoon's propagation speed. Experiment 5 uses a medium speed ($U < 8$ m s^{-1}) but the same category-1 Typhoon Utor (30 June–7 July 2001; ΔSST = 3.8°C) in place of Kai-Tak and yields ΔSST = 6.7°C. This is approximately double the Bender et al.'s (1993) criteria for the medium-moving storms (3.5°C) and confirms the relevance of the shallow thermocline particular to the summer of 2000 in producing the anomalously large ΔSST. Experiment 6 is the same as experiment 5, except that Utor's speed is artificially slowed to mimic Typhoon Kai-Tak. The ΔSST = 9.5°C is comparable to that induced by Kai-Tak. Thus, in addition to the unusual upper-ocean

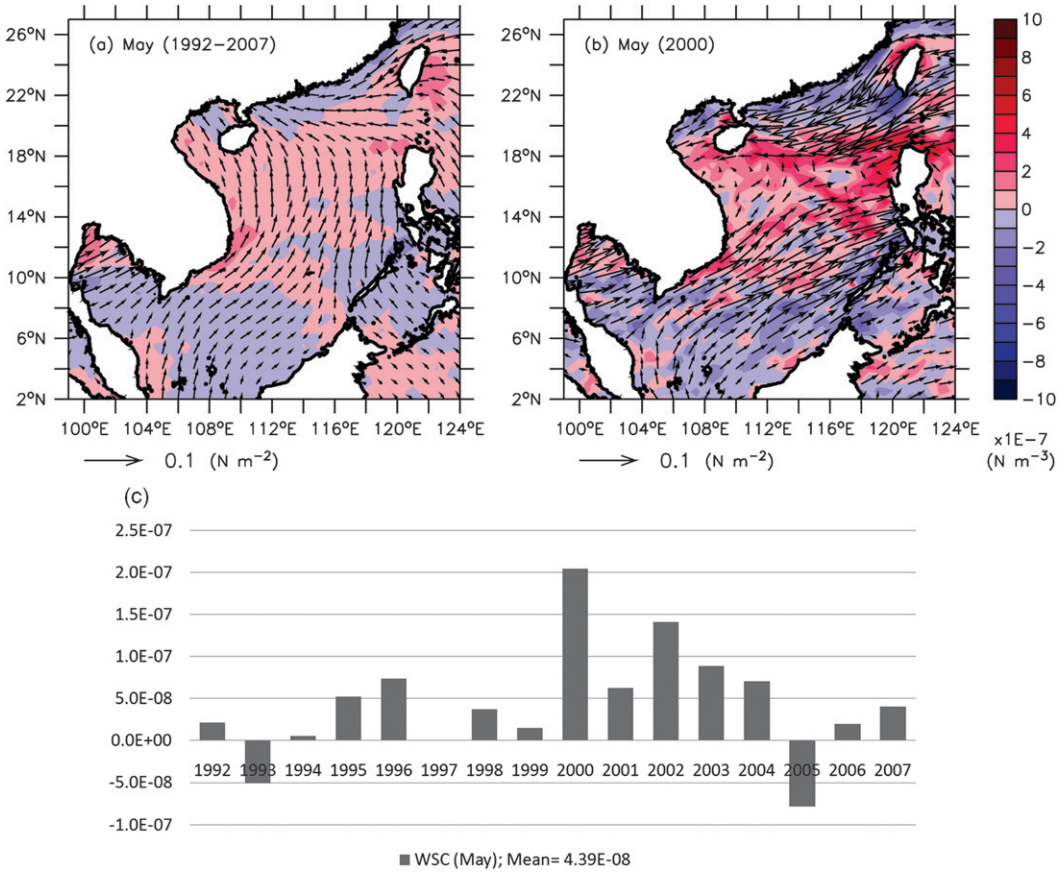

FIG. 7. (a) May climatological wind stress vectors superimposed on WSC (color); (b) as in (a), but for May 2000; (c) WSC (N m^{-3}) averaged over 16°–20°N and 116°–120°E for May from 1992 to 2007.

thermal structure, a slow-moving storm also contributes to the excessive surface cooling in summer 2000 during Kai-Tak.

4. Conditions for an ocean's perfect storm

Why were the main thermocline anomalously shallow and the sea surface anomalously warm prior to Kai-Tak (Fig. 6)? We now show how various components of the atmospheric and oceanic circulations in spring to early summer of 2000 fit together to create these favorable conditions for the extreme SST drop when Kai-Tak arrived.

May is a transition month of the East Asian monsoon. The climatological wind in the southern SCS south of approximately 16°N is from the west-southwest, whereas wind over the northern SCS still has the remnant of the winter monsoon and is from the east-northeast (Fig. 7a). In May 2000, the east-northeasterly wind was particularly strong (Fig. 7b). The wind stress magnitude exceeded 0.1 N m^{-2}, compared to a climatological value of approximately 0.04 N m^{-2}. The strong wind produced anomalously strong evaporative heat loss at the sea surface. The years 1999–2001 were La Niña years, but in May 2000 the strong heat loss contributed to the anomalously lower SSTs (Fig. 8a).

Figure 7c shows that, the maximum positive curl off the northwestern Luzon reaches $\sim 2 \times 10^{-7}$ N m^{-3} in 2000. This is more than ~5 times stronger than climatology ($\sim 4 \times 10^{-8}$ N m^{-3}) and is more typical of winter (January–March) values. Previous works (Qu 2000) have shown that a cyclonic eddy (the ''West Luzon Eddy'') at approximately (18°–19°N, 118°E) coincides well with the region of strong positive curl northwest of Luzon from late fall to early spring. Qu's (2000) maps of dynamic height show that the eddy appears in December and strengthens through the season until April when its center shifts northward to about the 19°N. The shift follows also a northward shift of the wind stress curl (WSC) and brings the eddy's center closer to the location of Kai-Tak's maximum ΔSST near 20°N, 119°E. However, because the eddy is large, ~300 km, the slight shift is not central to our argument. The important point here is that the positive wind stress curl correlates well with

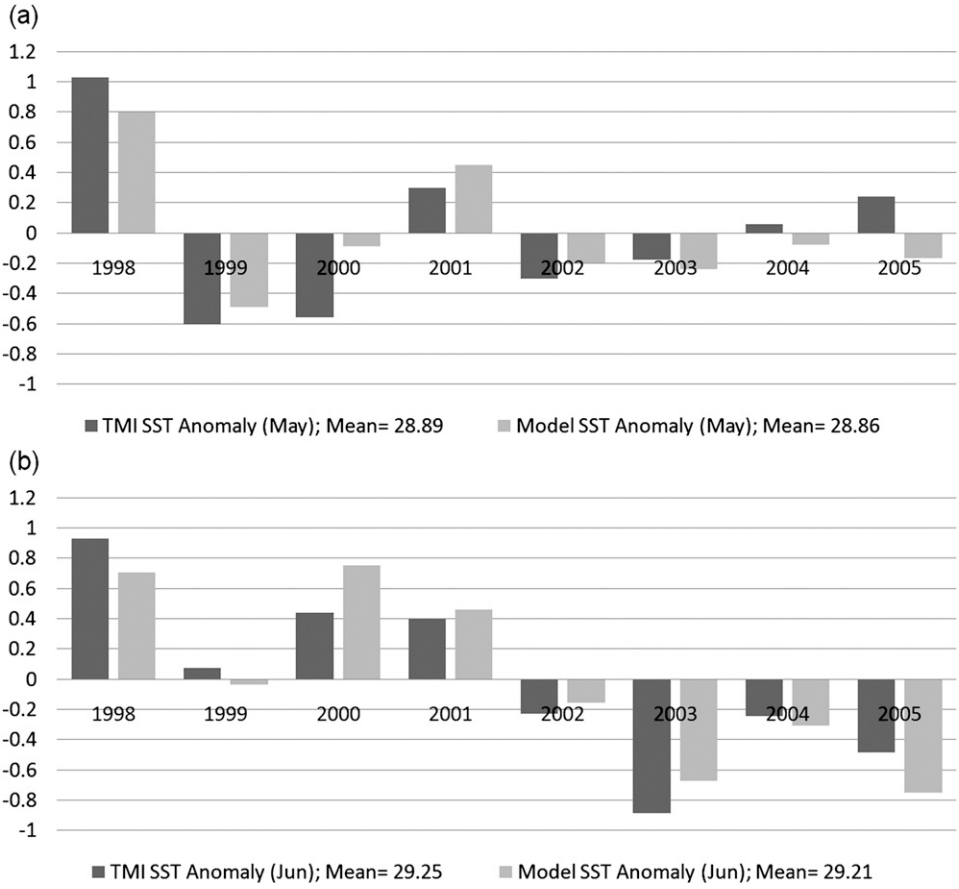

FIG. 8. The TMI and model SST anomalies (°C) averaged 3° × 3° at 20°N, 119°E for (a) May and (b) June from 1998 to 2005.

the West Luzon Eddy (Qu 2000). The eddy weakens in May–June. However, the anomalously strong wind stress curl in May 2000 prolongs the eddy's strength well into June prior to the arrival of Kai-Tak.

Qu's (2000) maps of dynamic height suggest also that the meridional current off the northwestern coast of Luzon can be taken as a measure of the strength of the West Luzon Eddy. Figure 9 shows anomalies of May wind stress curl representing forcing of the West Luzon Eddy and AVISO and model currents representing the eddy's strength. Except during the decaying phase of the strong 1997/98 El Niño and years of weak wind stress curl anomaly in 2001 and 2004, the west Luzon eddy is positively correlated with the wind stress curl. This result is consistent with Qu's (2000) findings. Moreover, the correlation between model and AVISO currents is high, ≈0.63, suggesting good model skill as it should be for wind-forced currents. In the year 2000, Fig. 9 clearly shows anomalously strong northward currents in 2000 coincident with the strong wind stress curl.

Figure 10 shows AVISO and model currents averaged over the last 2 weeks in June 2000 superimposed on the corresponding color maps of TMI SST. The northward flow northwest of Luzon, as well as the cyclonic eddy circulation, can be seen in both AVISO and model. The SST shows a band of warm water west of Luzon's coast that actually stretches farther south to approximately the 10°N (not shown); the warm water mass is clearly unrelated to the warm water east of Luzon in the Kuroshio. Liu et al. (2009) show that coastal waters west of Luzon warm up, generally in May, because of increased shortwave radiation in late spring and in combination with weak wind (because the west coast is in the wake of the northeasterly monsoon wind), resulting in reduced evaporative latent heat loss. Subsequently, northward and then westward offshore transport of this warm coastal water by the West Luzon Eddy clearly contributes to the presence of anomalously high SSTs to the north in June 2000 (Fig. 8b; there are also high SSTs during the onset of the 1998 La Niña and the weak La Niña of 2001). By 1 July 2000, prior to the arrival of Kai-Tak, a combination of the heat transport by the West Luzon Eddy, Ekman drift by southwesterly wind in June, and strong shortwave radiation resulted in

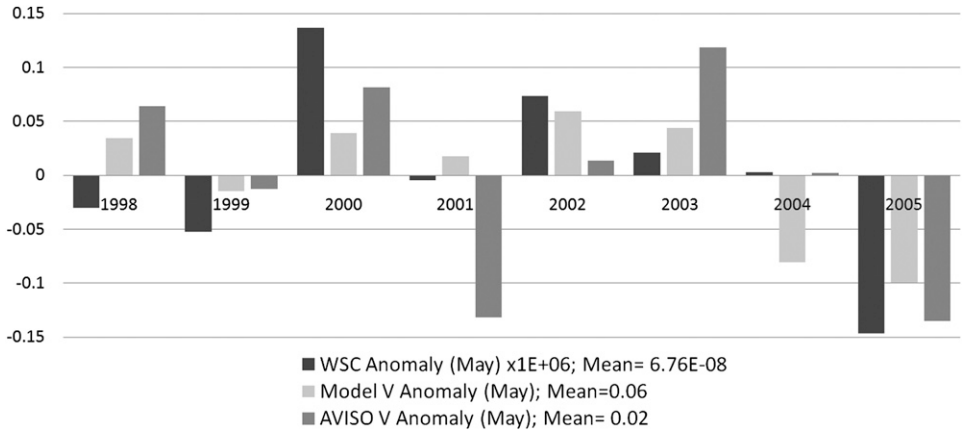

FIG. 9. May WSC anomaly (black bar; N m^{-3}) averaged over 16°–20°N and 116°–120°E and the anomalies of model upper 50 m (light shade) and AVISO (dark shade) meridional currents (m s^{-1}) averaged over 17°–19°N and 118°–120°E from 1998 to 2005.

very warm surface waters northwest of Luzon, clearly seen in the TMI SST image (Fig. 11).

In summary, the anomalously strong positive wind stress curl in late spring of 2000 spins up a strong West Luzon Eddy northwest of Luzon. The eddy lifts up isotherms and brings cool water nearer to the surface (Fig. 7). At the same time, the strong eddy also transports warm coastal waters west of Luzon northward and westward. Together with increased northward Ekman drift and solar radiation in early summer (June), an anomalously warm surface layer forms above the eddy. Figure 8 also shows that the high SSTs in June 2000 (Fig. 8b) is comparable to high SSTs during the onset of 1998 La Niña, whereas in May 2000 (Fig. 8a) the SSTs were considerably cooler because of the abnormally strong northeasterly monsoon wind in late spring of 2000. Northwest of Luzon, then, a cold subsurface eddy capped by a very warm surface layer was produced prior to the arrival of Typhoon Kai-Tak.

5. Conclusions

The present paper describes model simulation of intense surface cooling induced by Typhoon Kai-Tak (2000). The model reproduces well maximum SST drop and its location, as well as the area of intense surface cooling. By a careful design of model experiments, we successfully determine that 62% and 31% of the SST drop by Kai-Tak are caused by upwelling and entrainment, respectively. Kai-Tak belongs to a subcritical storm and upwelling dominates entrainment in producing the intense surface cooling. Moreover, because of the shallow

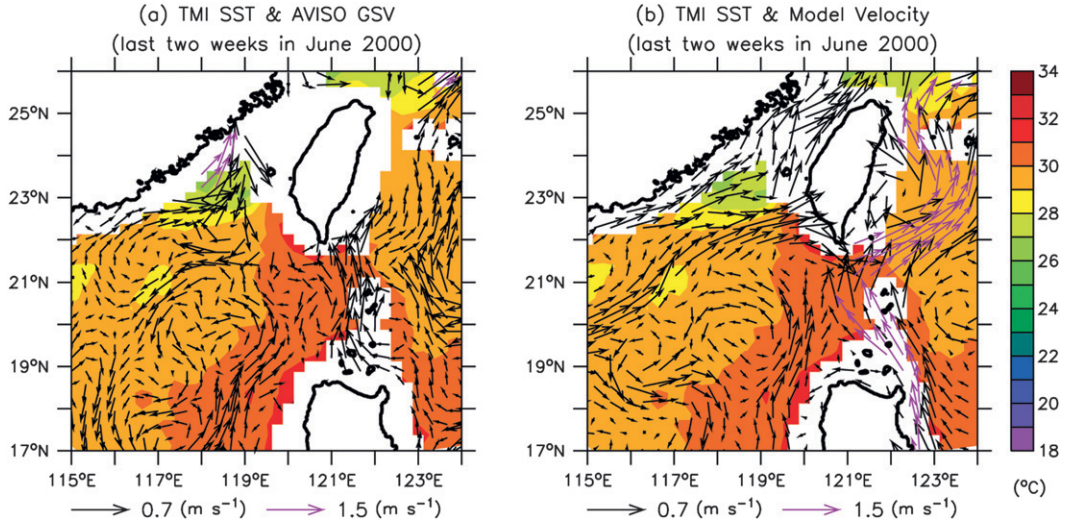

FIG. 10. (a) AVISO GSV and (b) upper 50-m model velocity superimposed on TMI SST of last 2 weeks in June 2000 (magenta vectors: a different scale for speeds >0.7 m s^{-1}).

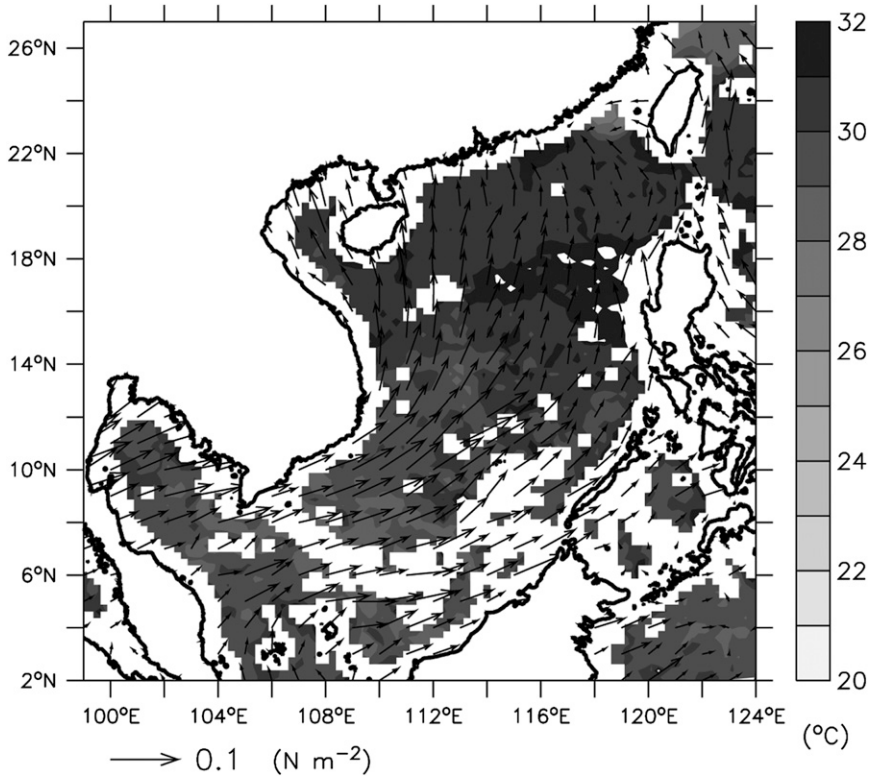

FIG. 11. Wind stress of June 2000 superimposed on TMI SST 3-day average image ending on 1 Jul 2000.

thermocline and correspondingly stronger stratification in summer of 2000, mixing contributes less SST drop than Ekman pumping. A unique combination of Kai-Tak's slow propagation speed and favorable climatic and oceanic conditions prior to the storm's arrival contributes to the large ΔSST. The unusually strong northeasterly monsoon wind over the northern SCS in spring of 2000, in combination with southwesterly wind in the southern SCS, spins an anomalously strong cyclonic wind stress curl hence also a strong west Luzon Eddy northwest of Luzon. The thermocline is uplifted near the eddy's center some 300 km northwest of Luzon, near 20°N, 119°E, where Kai-Tak passed. The eddy and Ekman drift by southerly wind in June also transport surface water northward along the Luzon west coast where strong solar radiation and weak winds produces anomalously warm SSTs. These climatic and oceanic processes created a cold eddy that was capped by a thin surface layer of anomalously warm water. Kai-Tak was the ocean's perfect storm in passing over the eddy at the ''right time,'' producing the record SST drop and high chlorophyll-a concentration.

Acknowledgments. We thank the two anonymous reviewers for their suggestions. C.-R. Wu is supported by the National Science Council, Taiwan, ROC, under Grants NSC 98-2111-M-003-002-MY2 and NSC 98-2628-M-003-001.

APPENDIX A

Effects of Thermocline Depth and a Typhoon's Propagation Speed

Experiments 3 and 4 (EX3 and EX4; see Table 1) were conducted to investigate the sensitivity of cooling because of different background fields (thermocline depths). Experiment 3 is initialized with the SCS model's 1 July 2001 field (instead of 1 July 2000). Kai-Tak forcing and other model parameters are the same. Figure A1a shows that the ΔSST pattern in EX3 is similar to that in CTL, but the maximum ΔSST is weaker, about 5.9°C. Experiment 4 is initialized with the June climatological temperature and salinity [*World Ocean Atlas 2001* (*WOA01*); Conkright et al. 2002] and spun up from rest for one month without wind forcing. It is then continued for another month forced by the Kai-Tak wind beginning on 23 June 2000 approximately one week before Kai-Tak. The ΔSST pattern (Fig. A1b) is also similar to that in CTL, and the maximum SST drop at the same location as for the CTL

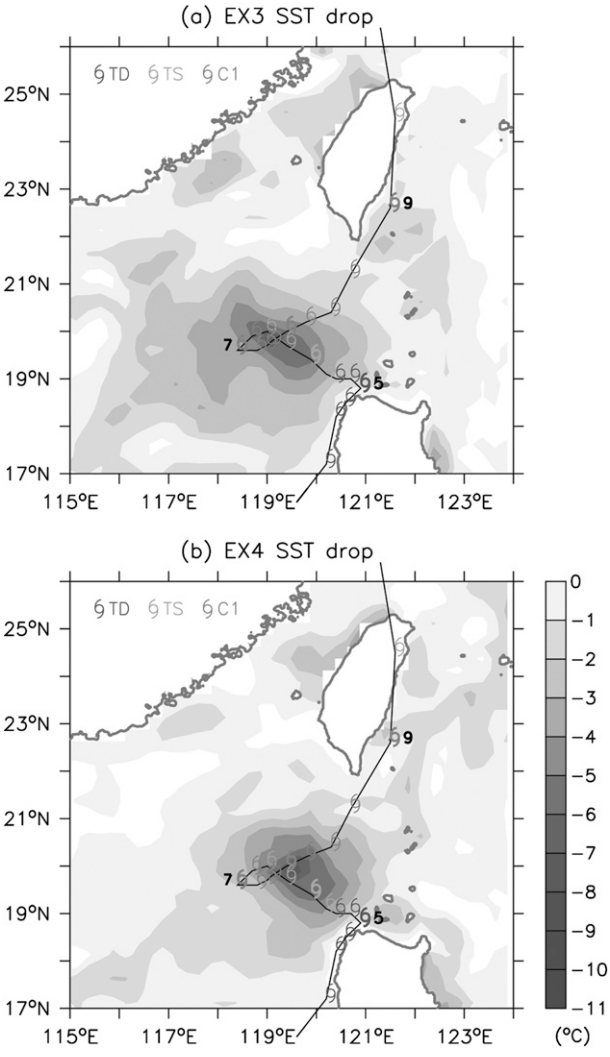

FIG. A1. SST drops for (a) EX3 and (b) EX4 between 2 and 9 Jul with Kai-Tak track with selected dates indicated and intensity from the JTWC best-track data.

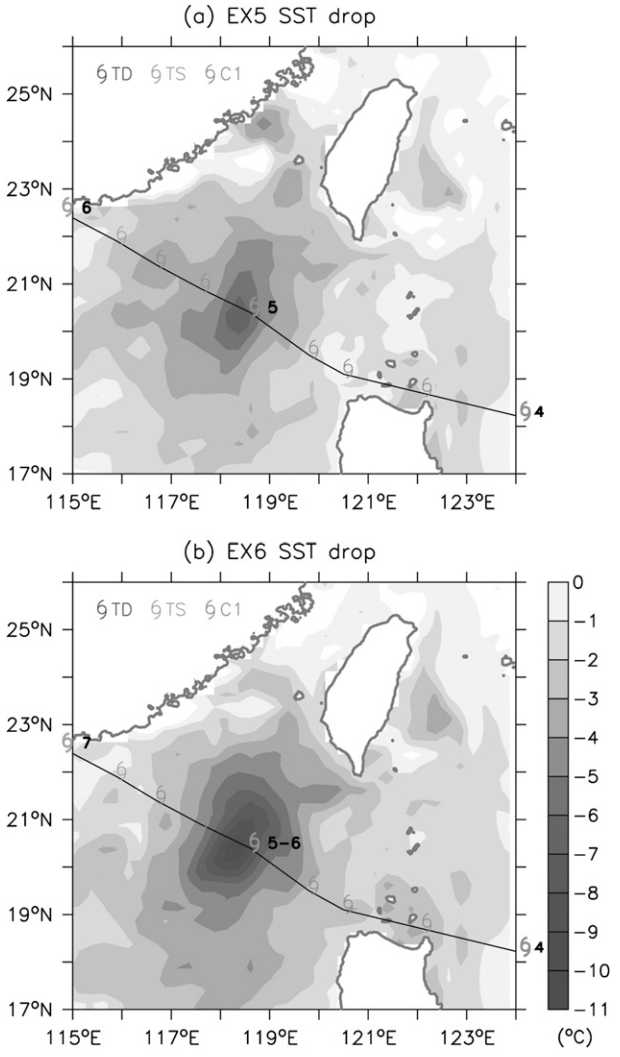

FIG. A2. SST drops for (a) EX5 between 3 and 7 Jul with Utor track and intensity from JTWC best-track data and (b) EX6 with 1-day stop track of Utor.

experiment is about 7.2°C. The ΔSSTs in both of these experiments are more than one standard deviation (2.03°C; Fig. 1) smaller than the ΔSST = 10.3°C of the CTL (Table 1). Because the only difference between CTL, EX3, and EX4 is the background temperature and salinity fields, in particular the different thermal structures, the above sensitivity tests show that the upper-ocean thermal structure during July 2000 (prior to Kai-Tak) is very different from climatology and also from other years.

To examine the effects of propagation speeds, we conduct two experiments both with the same background thermal (and salinity) fields as in summer 2000 (thinner D26 and colder seawater beneath) for Typhoon Kai-Tak, but we replace the wind field with that of Typhoon Utor (30 June–7 July 2001). Similarly to Kai-Tak, Utor is a category-1 typhoon with a maximum wind speed of 41.2 m s^{-1}. The storm also originated north of Luzon and during the first half of its life followed a northwestward path. It was a faster typhoon however ($U < 8$ m s^{-1}) during 5–6 July 2001, and the maximum SST drop was about 3.8°C; it therefore belongs to Bender et al.'s medium-speed category storm. In experiment 5 (EX5), Utor's wind is used, whereas in experiment 6 (EX6), Utor's propagation speed is artificially slowed (see below). The maximum SST cooling in EX5 is about 6.7°C (Fig. A2a), which is approximately double Bender et al.'s criteria for the medium-moving storms (3.5°C). Therefore, the thinner D26 and colder upper ocean can enhance typhoon-induced SST cooling. However, the SST drop in EX5 is still significantly lower than that induced by Kai-Tak, indicating that there are additional factors involved.

Experiment 6 (EX6; see Table 1) is the same as EX5, except that Utor's propagation is halted for 1 day on 5 July when the storm was near 20°N, 119°E (Fig. A2b). A ΔSST = 9.5°C is observed and comparable to that induced by Kai-Tak. The difference in ΔSST between EX5 and EX6 is purely caused by Utor's propagation speed in the two experiments. Because the initial thermal structure and other forcing are the same, they cannot contribute to the difference. Thus, in addition to the unusual upper-ocean thermal structure, a slow-moving storm contributes also to the excessive surface cooling in summer 2000 during Kai-Tak.

APPENDIX B

List of Acronyms

AVHRR	Advanced Very High Resolution Radiometer
AVISO	Archiving, Validation and Interpretation of Satellite Oceanographic data
D26	the depth of the 26°C isotherm
GSV	geostrophic velocity
JTWC	Joint Typhoon Warning Center
K_H	vertical diffusivity coefficient
K_M	vertical kinematic viscosity
NECP	National Centers for Environmental Prediction
POM	Princeton Ocean Model
QuikSCAT	Quick Scatterometer
SCS	South China Sea
SST	sea surface temperature
ΔSST	SST drop
TC	tropical cyclone
TCWPM	Tropical Cyclone Wind Profile Model
TMI	Tropical Rainfall Measuring Mission Microwave Imager
U	propagation speed
WOA01	*World Ocean Atlas 2001*

REFERENCES

Bender, M. A., I. Ginis, and Y. Kurihara, 1993: Numerical simulations of tropical cyclone-ocean interaction with a high-resolution coupled model. *J. Geophys. Res.,* **98** (D12), 23 245–23 263.

Chiang, T.-L., C.-R. Wu, and S.-Y. Chao, 2008: Physical and geographical origins of the South China Sea Warm Current. *J. Geophys. Res.,* **113,** C08028, doi:10.1029/2008JC004794.

Chu, P. C., J. M. Veneziano, C. Fan, M. J. Carron, and W. T. Liu, 2000: Response of the South China Sea to Tropical Cyclone Ernie 1996. *J. Geophys. Res.,* **105** (C6), 13 991–14 009.

Conkright, M. E., R. A. Locarnini, H. E. Garcia, T. D. O'Brien, T. P. Boyer, C. Stephens, and J. I. Antonov, 2002: *World Ocean Atlas 2001: Objective Analyses, Data Statistics, and Figures.* National Oceanographic Data Center, 17 pp.

Geisler, J. E., 1970: Linear theory of the response of a two layer ocean to a moving hurricane. *Geophys. Fluid Dyn.,* **1,** 249–272, doi:10.1080/03091927009365774.

Hsin, Y.-C., C.-R. Wu, and P.-T. Shaw, 2008: Spatial and temporal variations of the Kuroshio east of Taiwan, 1982–2005: A numerical study. *J. Geophys. Res.,* **113,** C04002, doi:10.1029/2007JC004485.

Jiang, X. P., Z. Zhong, and J. J. Jiang, 2009: Upper ocean response of the South China Sea to Typhoon Krovanh (2003). *Dyn. Atmos. Oceans,* **47** (1–3), 165–175, doi:10.1016/j.dynatmoce.2008.09.005.

Large, W. G., and S. Pond, 1981: Open ocean momentum flux measurements in moderate to strong winds. *J. Phys. Oceanogr.,* **11,** 324–336.

Lin, I.-I., and Coauthors, 2003: New evidence for enhanced ocean primary production triggered by tropical cyclone. *Geophys. Res. Lett.,* **30,** 1718, doi:10.1029/2003GL017141.

Liu, Q., C. Sun, and X. Jiang, 2009: Formation of spring warm water southwest of the Philippine Islands: Winter monsoon wake effects. *Dyn. Atmos. Oceans,* **47,** 154–164, doi:10.1016/j.dynatmoce.2008.08.003.

Mellor, G. L., 2004: Users guide for a three-dimensional, primitive equation, numerical ocean model. Princeton University Program in Atmosphere and Oceanic Sciences Manual, 56 pp.

Milliff, R. F., W. G. Large, J. Morzel, G. Danabasoglu, and T. M. Chin, 1999: Ocean general circulation model sensitivity to forcing from scatterometer winds. *J. Geophys. Res.,* **104** (C5), 11 337–11 358.

Oey, L.-Y., T. Ezer, D.-P. Wang, S.-J. Fan, and X.-Q. Yin, 2006: Loop Current warming by Hurricane Wilma. *Geophys. Res. Lett.,* **33,** L08613, doi:10.1029/2006GL025873.

——, ——, ——, X.-Q. Yin, and S.-J. Fan, 2007: Hurricane-induced motions and interaction with ocean currents. *Cont. Shelf Res.,* **27,** 1249–1263, doi:10.1016/j.csr.2007.01.008.

——, M. Inoue, R. Lai, X.-H. Lin, S. Welsh, and L. Rouse Jr., 2008: Stalling of near-inertial waves in a cyclone. *Geophys. Res. Lett.,* **35,** L12604, doi:10.1029/2008GL034273.

Powell, M. D., P. J. Vickery, and T. A. Reinhold, 2003: Reduced drag coefficient for high wind speeds in tropical cyclones. *Nature,* **422,** 279–283, doi:10.1038/nature01481.

Price, J. F., 1981: Upper ocean response to a hurricane. *J. Phys. Oceanogr.,* **11,** 153–175.

Qu, T., 2000: Upper-layer circulation in the South China Sea. *J. Phys. Oceanogr.,* **30,** 1450–1460.

Trenberth, K. E., 1989: Surface wind stress from global atmospheric analyses. *Proc. Oceans '89,* Seattle, WA, IEEE, Vol. 1, 254–259.

Wentz, F. J., C. Gentemann, D. Smith, and D. Chelton, 2000: Satellite measurements of sea surface temperature through clouds. *Science,* **288,** 847–850, doi:10.1126/science.288.5467.847.

Wu, C.-R., and T.-L. Chiang, 2007: Mesoscale eddies in the northern South China Sea. *Deep-Sea Res. II,* **54,** 1575–1588, doi:10.1016/j.dsr2.2007.05.008.

——, Y.-L. Chang, L.-Y. Oey, C.-W. J. Chang, and Y.-C. Hsin, 2008: Air-sea interaction between Tropical Cyclone Nari and Kuroshio. *Geophys. Res. Lett.,* **35,** L12605, doi:10.1029/2008GL033942.

Yablonsky, R. M., and I. Ginis, 2009: Limitation of one-dimensional ocean models for coupled hurricane–ocean model forecasts. *Mon. Wea. Rev.,* **137,** 4410–4419.